Analysis of the Dynamics of Gelation in Polymerization Reactors Using the "Numerical Fractionation" Technique

F. Teymour*

Department of Chemical Engineering, Illinois Institute of Technology, Chicago, Illinois 60616

J. D. Campbell

S. C. Johnson Polymer, Racine, Wisconsin 53403

Received July 16, 1993; Revised Manuscript Received November 15, 1993®

ABSTRACT: A dynamic model for the molecular weight properties of polymers with potential gel formation is constructed based on the "Numerical Fractionation" technique. This technique, introduced earlier, relies on the numerical segregation of the polymer population into a series of unimodal subdistributions of similar structure and size. The concepts leading to its derivation provide a new framework in which gelation can be explained. The phenomena accompanying the molecular weight divergence at the gel point are found to be related to heterogeneities in the polymer microstructure. The method presented allows for the computation of sol properties, gel fraction, the gel point, and the reconstruction of the molecular weight distribution. The discontinuity in molecular weight moments at the gel point is avoided by this method, and thus continuous integration through the gel point is possible. Sol properties in the postgel regime can also be computed since the definition of polymer generations allows for the numerical separation of sol and gel at all times. Finally, the method provides a criterion for *a priori* determination of the potential for gelation of any specific reaction mechanism.

Introduction

Since the early days of polymer manufacture, branched and cross-linked polymers have been of considerable commerical importance. Examples include the synthetic rubbers (*e.g.*, polyisoprene, styrene–butadiene rubber (SBR), ...). However, the manufacture of these polymers had to be crafted into an art, because of the frustrations resulting from potential gel formation and the lack of mechanistic understanding of this phenomenon. It was only through the pioneering efforts of Flory[1] and Stockmayer[2] that a new understanding of the nature of gel and the sol/gel transition was obtained. Their classical theory used a statistical approach and was limited to stepwise polymerization systems. Equivalent theories were later proposed and extended to addition polymerization systems independently by Gordon[3] and by Macosko and Miller.[4] More recent applications to these systems include those of Dotson *et al.*[5] and Scranton and Peppas;[6] however, statistical methods have not had as much success with addition polymerization systems as with step-growth systems. This results primarily from the complexity of derivations of these models and from their lack of adaptability to describing reactor dynamics, especially in the continuous case. The kinetic approach based on the method of moments is usually more suitable for this task and has been successfully applied to the analysis of the molecular weight dynamics of branched polymers.[7-10] However, this approach fails in the vicinity of the gel point as a result of the divergence of the second and higher moments of the molecular weight distribution at this point, an inherent feature of the gelation process. Recently, Tobita and Hamielec[11] proposed a postgel modeling technique using a kinetic equation for the gel formation but had to use a generalized form of Flory's statistical theory for cross-linked polymers to obtain initial conditions for their model at the gel point. Charmot and Guillot[12] used an approach based on the instantaneous primary chain distribution, thus differentiating between sol and gel according to the number of cross-links per primary chain. Although their results are insensitive to whether this number is 2 or 3, the fundamental basis of this criterion is not obvious. Their model predictions compared favorably with experimental results for styrene–butadiene emulsion polymerization and with the model of Tobita and Hamielec.

Percolation theory approaches have been used extensively to model possible deviations from the classical Flory–Stockmayer theory, as, *e.g.*, by Stauffer.[13] Various degrees of success have been achieved by more recent applications of these methods,[14-18] which typically provide useful information on the microstructure and connectivity of the polymer chains, but have not proven useful for the purpose of polymerization reactor design and dynamic analysis. These also usually require Monte Carlo type simulations which are very demanding of computer time. Recently, Bowman and Peppas[19] have presented a kinetic simulation for the gelation behavior of tetrafunctional homopolymerization using a face-centered-cubic lattice.

In this paper, we propose a new theory to describe the nature of the progression to gelation, and we present a relative simple modeling technique that overcomes the difficulties detailed above. The method uses the kinetic approach but is not limited to calculating the moments of the overall polymer population. Instead, it identifies a succession of branched polymer generations that evolve en route to gelation and are modeled individually. The method provides new insight into the sol/gel transition and results in a wide spectrum of information from a single model. The concepts leading to the formulation of this method and details about its derivation are presented in what follows. The term "Numerical Fractionation", introduced in an earlier publication,[20] refers to the numerical isolation of various polymer generations based on the degree of complexity of their microstructure, as will be detailed later.

Concepts and Methodology

Before we can introduce the proposed modeling technique properly, we have to discuss a few aspects of gelation

* Author to whom correspondence should be addressed.
® Abstract published in *Advance ACS Abstracts*, March 15, 1994.

0024-9297/94/2227-2460$04.50/0

that are essential to its development. Gel molecules are usually thought of as polymer networks of infinite length, because of the vast difference in scale that separates them from normal sol polymer molecules. It is because of this difference in scale that a fractal description is most suitable for analyzing gel, as is commonly acknowledged by the percolation theory approach. It is this fractal nature of gel, along with the processes leading to its formation, that are addressed by the theory presented here. To gain a better understanding of this, one might resort to an analogous example from the field of particle agglomeration, where two modes of particle growth are generally recognized:[21] one in which fine powders attach themselves to an agglomerate or cluster and the other where two or more clusters aggregate directly. It is this cluster–cluster agglomeration process that will lead to a rapid geometric change of scale and thus form aggregates with properties that are vastly different from those of their parent particles. The theory presented here necessitates the presence of polymer growth mechanisms equivalent to this type of agglomeration process in order for gelation to occur, as detailed in what follows.

In the method used, not only is the overall polymer population divided into linear and branched fractions but also the latter is further subdivided into various branched polymer generations. These generations will be generally composed of polymer molecules that are similar in scale (or degree of clustering) by virtue of the processes through which they were formed. As one moves from one generation to the next the average molecular size will grow geometrically, thus leading (at least theoretically) toward a generation of infinitely large polymer molecules. It is this limit that actually represents gelation and that we aim to isolate. First, let us examine what occurs as a polymerizing system progresses toward gelation. In the early stages, linear polymer predominates; then, if branching reactions exist, some branched polymer will form; we shall refer to the latter as a first-generation branched polymer. The polymer in this generation will keep adding branches and strands of linear polymer yet will still be considered to belong to this same generation. Transfer to the second generation will only occur if two first-generation members connect together forming a single polymer molecule. This resulting molecule will consequently add more first-generation and linear polymer before it finally reacts with another second-generation member (or higher) and transfers to a higher generation. In this respect, each generation of branched polymer can be seen to provide the building blocks for the next higher generation, as sand particles can be made into bricks, bricks into buildings, buildings into communities, communities into cities, and so on. This mechanism imparts into the larger molecules a certain degree of self-similarity which results in a fractal microstructure for these polymer molecules.

As a result of this growth process higher generations keep appearing in succession but always in smaller amounts since less and less of the younger generations will be available to form them. After a number of such transitions, the resulting polymer will be large enough that gel suddenly appears and the gel/sol transition occurs. (This behavior bears a strong similarity to the appearance of chaos in dynamical systems via a succession of period-doubling bifurcations, a fact that will be touched upon elsewhere.) Shortly thereafter, the newly formed gel molecules start reacting with the sol polymer, consuming the higher generations first since the rate of most cross-linking reactions depends on molecular size. As a result, these higher generations can be seen to be transient in nature,

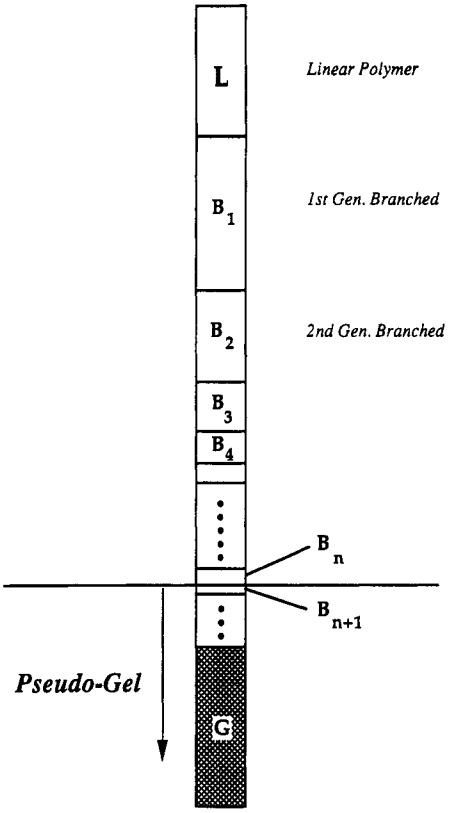

Figure 1. Concept of pseudogel. The sol polymer is fractionated into one linear generation and n branched generations; all higher generations are lumped with the actual gel to represent a pseudogel.

since they only appear shortly before the gel point is reached and then are consumed immediately after. It is this feature of the higher generations that allows us to effectively approximate the gel and sol populations without any considerable loss of information. It will be generally sufficient to keep track of a finite number of branched generations and consider all higher generations plus any gel formed to constitute a "pseudogel", as illustrated in Figure 1. This approximation will only be in error in the immediate vicinity of the gel point, and even then the error will be minimal if an adequate number of generations is utilized (5–10 is usually sufficient).

It is also instructive to consider how the molecular weight distribution (MWD) evolves en route to gelation. During the early stages of polymerization the MWD represents mostly linear polymer and thus approaches the most probable distribution with a polydispersity index of 1.5–2.0 (depending on the mode of termination). When sufficient branched polymer forms, the overall MWD will consist of the sum of two unimodal distributions (linear and branched) with different average molecular weights. Thus, a shoulder usually appears near the high-MW end of the distribution, signifying the presence of multiple populations in the polymer mixture and resulting in an increase in polydispersity. Each new generation of branched polymer keeps adding a shoulder or a peak to that high end of the distribution as it appears, and the tail of the MWD keeps extending toward larger molecular weights. As gelation occurs the end of the MWD snaps off and forms gel (at molecular weights beyond computational capabilities), and the tail of the remaining sol MWD starts moving back toward lower values of MW. Shortly after gelation only the sol MWD (which can be highly polydisperse at this point) and that of the gel (assumed to be at infinity) remain; the transient species talked about earlier would have disappeared at this point.

This process explains the behavior of the sol polydispersity which increases toward infinity as the gel point is approached and then starts decreasing afterward, as discussed by Flory.[1] It also explains the reason behind the failure of the kinetic approach based on the moments of the overall polymer distribution; it attempts to lump the sol and gel polymer molecules in the same population despite the vast difference in their size scales.

Mathematical Model

In this section, a mathematical model is derived for a case study where long-chain branching results from chain transfer to polymer. Both termination mechanisms (combination and disproportionation) are included, as well as chain transfer to the monomer and solvent species. Modification to account for other branching mechanisms should follow similar steps and is straightforward. The method of moments is used and is applied to each generation individually. The rules of transfer between generations have to be adhered to, namely, that transfer to the next higher generation only results if a connecting reaction (*e.g.*, termination by combination, reaction with a pendant, internal or terminal double bond, ...) occurs between two molecules in the same generation. If the reaction is between molecules of dissimilar generations, the resulting polymer always belongs to the higher generation. The only exception to these rules are for transfer between the linear generation and the first branched generation, since the combination of two linear radicals results in a linear polymer chain. Thus transfer away from the linear polymer generation will only occur when branching takes place (*e.g.*, via chain transfer to polymer), and in this case a linear dead polymer chain immediately transforms into a first-generation branched radical.

The following notation is used for the different species involved: For live radicals, $R_{0,r}$ = linear radical of length r, $R_{i,r}$ = branched radical of length r in generation i (i = 1, ..., n), ρ_{ij} = jth live moment for generation i (i = 0 for linear), and Y_j = jth overall live moment. For dead polymer, L_r = linear polymer of length r, $B_{i,r}$ = branched polymer of length r in generation i, G_r = pseudogel polymer, λ_j = jth dead moment for linear polymer, β_{ij} = jth dead moment for branched generation i, γ_j = jth dead moment for pseudogel, and Q_j = jth overall dead moment.

Overall Polymer Moments. The overall moments are given by the traditional equations that result from applying the method of moments to balance equations on the overall live and dead polymer populations, as presented, for example, by Tobita and Hamielec.[10] The definition of the various moments of the MWD is also provided by these authors.

The overall live moments are given by:

$$Y_0 = \left(\frac{\mathcal{R}_i}{k_{t_c} + k_{t_d}}\right)^{1/2} \tag{1}$$

$$Y_1 = \frac{1 + \tau + \beta + C_p Q_2}{\tau + \beta + C_p Q_1} Y_0 \tag{2}$$

where $\mathcal{R}_i$ denotes the rate of initiation and τ, β, and C_p are given by:

$$\tau = \frac{k_{t_d} Y_0 + k_{f_m}[M] + k_{f_s}[S]}{k_p[M]} \qquad \beta = \frac{k_{t_c} Y_0}{k_p[M]} \qquad C_p = \frac{k_{f_p}}{k_p[M]}$$

In addition, the overall dead polymer moments can be expressed as:

$$\frac{dQ_0}{dt} = k_p[M] Y_0 \left(\tau + \frac{\beta}{2} - (1 - \phi) C_p Q_1\right) \tag{3}$$

$$\frac{dQ_1}{dt} = k_p[M] Y_0 (1 + \phi\tau + \beta - (1 - \phi) C_p Q_1) \tag{4}$$

where ϕ is the probability of propagation given by:

$$\phi = \frac{1}{1 + \tau + \beta + C_p Q_1} \tag{5}$$

The overall second moment is not used in our formulation, since it is known to diverge at the gel point. The methodology used characterizes the gel point by calculating the gel fraction.

Live Polymer Moments. In order to derive the polymer moments for each generation of live radicals, we start by formulating radical population balances for each generation, and then we apply the method of moments to these.

A population balance for linear radicals can be formulated as:

$$\frac{dR_{0,r}}{dt} = k_p[M] R_{0,r-1} - \{k_p[M] + (k_{t_c} + k_{t_d}) Y_0 + k_{f_m}[M] + k_{f_s}[S] + k_{f_p} Q_1\} R_{0,r} + \delta\{(k_{f_s}[S] + k_{f_m}[M]) Y_0 + \mathcal{R}_i\} \tag{6}$$

where $\delta = 1$ for $r = 1$ and $\delta = 0$ for $r > 1$.

This could be simplified as:

$$\frac{dR_{0,r}}{dt} = k_p[M]\{R_{0,r-1} - (1 + \tau + \beta + C_p Q_1) R_{0,r} + \delta(\tau + \beta) Y_0\} \tag{7}$$

Similarly, a balance on branched radicals in the first generation will result in:

$$\frac{dR_{1,r}}{dt} = k_p[M]\{R_{1,r-1} - (1 + \tau + \beta + C_p Q_1) R_{1,r} + C_p Y_0 [r L_r + r B_{1,r}]\} \tag{8}$$

and a balance for the general ith generation results in:

$$\frac{dR_{i,r}}{dt} = k_p[M]\{R_{i,r-1} - (1 + \tau + \beta + C_p Q_1) R_{i,r} + C_p Y_0 r B_{i,r}\} \tag{9}$$

Notice that these equations assume that chain transfer to a linear polymer chain results in a first-generation branched radical, whereas transfer to any other generation of polymer results in a radical belonging to the same generation.

Taking the moments of eqs 7–9 and applying the quasi-steady-state approximation (QSSA) for live radicals result in the following live radical moments:

1. linear live moments

$$\rho_{0,0} = \left(\frac{\tau+\beta}{\tau+\beta+C_pQ_1}\right)Y_0 \tag{10}$$

$$\rho_{0,1} = \left(\frac{1+\tau+\beta+C_pQ_1}{\tau+\beta+C_pQ_1}\right)\rho_{0,0} \tag{11}$$

$$\rho_{0,2} = \left(\frac{2+\tau+\beta+C_pQ_1}{\tau+\beta+C_pQ_1}\right)\rho_{0,1} \tag{12}$$

2. first-generation branched

$$\rho_{1,0} = \frac{C_p(\lambda_1+\beta_{1,1})Y_0}{\tau+\beta+C_pQ_1} \tag{13}$$

$$\rho_{1,1} = \frac{\rho_{1,0}+C_p(\lambda_2+\beta_{1,2})Y_0}{\tau+\beta+C_pQ_1} \tag{14}$$

$$\rho_{1,2} = \frac{\rho_{1,0}+2\rho_{1,1}+C_p(\lambda_3+\beta_{1,3})Y_0}{\tau+\beta+C_pQ_1} \tag{15}$$

3. *i*th-generation branched

$$\rho_{i,0} = \frac{C_p\beta_{i,1}Y_0}{\tau+\beta+C_pQ_1} \tag{16}$$

$$\rho_{i,1} = \frac{\rho_{i,0}+C_p\beta_{i,2}Y_0}{\tau+\beta+C_pQ_1} \tag{17}$$

$$\rho_{i,2} = \frac{\rho_{i,0}+2\rho_{i,1}+C_p\beta_{i,3}Y_0}{\tau+\beta+C_pQ_1} \tag{18}$$

Dead Polymer Moments. The derivation of dead polymer moments follows steps similar to those for the live polymer. The main rule governing transfer between generations is that a polymer chain is transferred to the next generation only if it connects with another member of the same generation, whereas, if it connects with a higher generation chain, the resulting chain will belong to the higher generation. The starting point for the derivation is again the formulation of population balances for the various polymer generations. Linear-chains are thus described by:

$$\frac{dL_r}{dt} = \frac{k_{t_c}}{2}\sum_{s<r}R_{0,s}R_{0,r-s} + k_zR_{0,r} - k_{f_p}Y_0rL_r \tag{19}$$

where k_z is defined by:

$$k_z = k_{f_m}[M] + k_{f_s}[S] + k_{f_p}Q_1 + k_{t_d}Y_0$$

Similarly, balances on first- and *i*th-generation branched polymer result in:

$$\frac{dB_{1,r}}{dt} = k_{t_c}\sum_{s<r}R_{1,s}R_{0,r-s} + k_zR_{1,r} - k_{f_p}Y_0rB_{1,r} \tag{20}$$

$$\frac{dB_{i,r}}{dt} = k_{t_c}\sum_{s<r}R_{i,s}\left(\sum_{j=0}^{i-1}R_{j,r-s}\right) + \frac{k_{t_c}}{2}\sum_{s<r}R_{i-1,s}R_{i-1,r-s} + k_zR_{i,r} - k_{f_p}Y_0rB_{i,r} \tag{21}$$

Lastly, a population balance on the pseudogel species (all generations beyond the *n*th generation) results in:

$$\frac{dG_r}{dt} = k_zR_{n+1,r} - k_{f_p}Y_0rG_r + k_{t_c}\sum_{s<r}R_{n+1,s}\left(\sum_{j=0}^{n}R_{j,r-s}\right) + \frac{k_{t_c}}{2}\sum_{s<r}(R_{n,s}R_{n,r-s} + R_{n+1,s}R_{n+1,r-s}) \tag{22}$$

Notice that in eq 22 $R_{n+1,r}$ denotes a pseudogel radical of length r.

Applying the method of moments to the above equations results in the following moment balances:

1. linear dead polymer moments

$$\frac{d\lambda_0}{dt} = k_z\phi\rho_{0,0} + \frac{k_{t_c}}{2}\rho_{0,0}^2 - k_{f_p}Y_0\lambda_1 \tag{23}$$

$$\frac{d\lambda_1}{dt} = k_z[\rho_{0,1} - (1-\phi)\rho_{0,0}] + k_{t_c}\rho_{0,0}\rho_{0,1} - k_{f_p}Y_0\lambda_2 \tag{24}$$

$$\frac{d\lambda_2}{dt} = k_z[\rho_{0,2} - (1-\phi)\rho_{0,0}] + k_{t_c}(\rho_{0,1}^2 + \rho_{0,0}\rho_{0,2}) - k_{f_p}Y_0\lambda_3 \tag{25}$$

2. first-generation branched

$$\frac{d\beta_{1,0}}{dt} = k_z\rho_{1,0} + k_{t_c}\rho_{1,0}\rho_{0,0} - k_{f_p}Y_0\beta_{1,1} \tag{26}$$

$$\frac{d\beta_{1,1}}{dt} = k_z\rho_{1,1} + k_{t_c}(\rho_{1,0}\rho_{0,1} + \rho_{1,1}\rho_{0,0}) - k_{f_p}Y_0\beta_{1,2} \tag{27}$$

$$\frac{d\beta_{1,2}}{dt} = k_z\rho_{1,2} + k_{t_c}(\rho_{1,2}\rho_{0,0} + 2\rho_{1,1}\rho_{0,1} + \rho_{1,0}\rho_{0,2}) - k_{f_p}Y_0\beta_{1,3} \tag{28}$$

3. *i*th-generation branched

$$\frac{d\beta_{i,0}}{dt} = k_z\rho_{i,0} + k_{t_c}\rho_{i,0}\left(\sum_{j<i}\rho_{j,0}\right) + \frac{k_{t_c}}{2}\rho_{i-1,0}^2 - k_{f_p}Y_0\beta_{i,1} \tag{29}$$

$$\frac{d\beta_{i,1}}{dt} = k_z\rho_{i,1} + k_{t_c}\left[\rho_{i,0}\left(\sum_{j<i}\rho_{j,1}\right) + \rho_{i,1}\left(\sum_{j<i}\rho_{j,0}\right)\right] + k_{t_c}\rho_{i-1,0}\rho_{i-1,1} - k_{f_p}Y_0\beta_{i,2} \tag{30}$$

$$\frac{d\beta_{i,2}}{dt} = k_z\rho_{i,2} + k_{t_c}\left[\rho_{i,2}\left(\sum_{j<i}\rho_{j,0}\right) + 2\rho_{i,1}\left(\sum_{j<i}\rho_{j,1}\right) + \rho_{i,0}\left(\sum_{j<i}\rho_{j,1}\right)\right] + k_{t_c}[\rho_{i-1,1}^2 + \rho_{i-1,0}\rho_{i-1,2}] - k_{f_p}Y_0\beta_{i,3} \tag{31}$$

One could also derive equations for the zeroth and first moments of the pseudogel generation; however, numerical difficulties will result when these are used. Instead, these moments are calculated by difference after subtracting the sum of a particular moment over all generations from the corresponding overall moment. In any instance, only the first moment of the pseudogel can be calculated accurately; however, this is still very useful since it provides a measure of the gel fraction after the gel point.

Equations 23–31 indicate the emergence of a closure problem for the individual generation moments, since every moment depends on the next higher. This was resolved by using the Saidel and Katz[8] approximation for the third moment.

This approximation was found adequate since each generation possesses a unimodal distribution as ensured

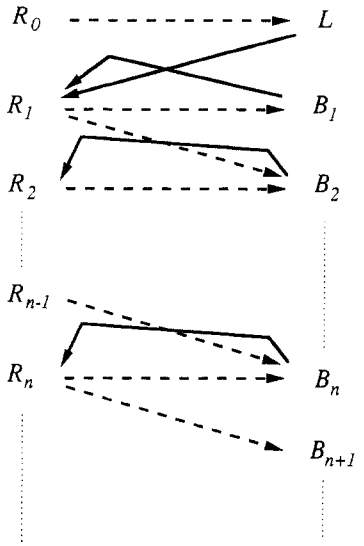

Figure 2. Generation transfer chart for the reaction mechanism used. R_i, L, and B_i represent live radicals, linear dead polymer, and branched dead polymer, respectively. (→) Chain transfer to polymer. (- - →) Termination.

by the fractionation approach. It should be noted that this closure problem appears only for the generation moments and not for the overall moments, which thus require no approximation. The resulting representation of any given third moment is given by:

$$Q_3 = 2\frac{Q_2^2}{Q_1} - \frac{Q_2 Q_1}{Q_0} \tag{32}$$

The model thus derived is comprised of a set of ordinary differential equations (ODEs) describing the dead polymer moments, complemented by a set of explicit algebraic equations for the live polymer moments. The number of equations solved depends on the number of branched generations selected. For the case of n branched generations, the model will consist of "$3n$ + 5" ODEs and "$3n$ + 5" algebraic equations. These equations were solved using a software package (DASSL[22]) for the numerical solution of ordinary differential equation systems.

Results and Discussion

It is obvious from the above discussion that gel formation requires the presence of a branching mechanism and a connection mechanism. The latter can now be seen to be any reaction between polymeric species that results in a net decrease in the number of polymer molecules. In this section, we will apply our method to an isothermal batch polymerization reactor where branching occurs as a result of chain transfer to polymer and where live radical termination proceeds via combination; this same example was analyzed by Tobita and Hamielec[10] and will be used here to illustrate our method. The parameters used in this example are such that $\tau_0 = 1 \times 10^{-4}$, $\beta_0 = 1 \times 10^{-5}$, and $\epsilon = k_{fp}/k_p = 1 \times 10^{-3}$. Later in this section, we will analyze an example where termination is solely by disproportionation, to illustrate the necessity of the combination step for the occurrence of gelation in this polymerization mechanism.

The branching and connection reactions of this mechanism are illustrated in Figure 2, where these reactions can be seen to lead to the transfer of polymer chains between the polymer generations defined earlier. This kind of generation transfer chart provides an effective way for *a priori* detection of the possibility of gelation for any reaction mechanism. The simple criterion is that for gelation to occur there must exist a reaction path cascading down the generations and enabling the formation of pseudogel. Any mechanism lacking such a reaction step cannot possibly lead to gelation, as will be shown later. However, the converse is not guaranteed, making this a necessary but not sufficient condition for gelation. Existence of such a reaction path will ensure that a geometric growth process can be obtained, resulting in the formation of polymer networks of vast proportions and enabling gelation.

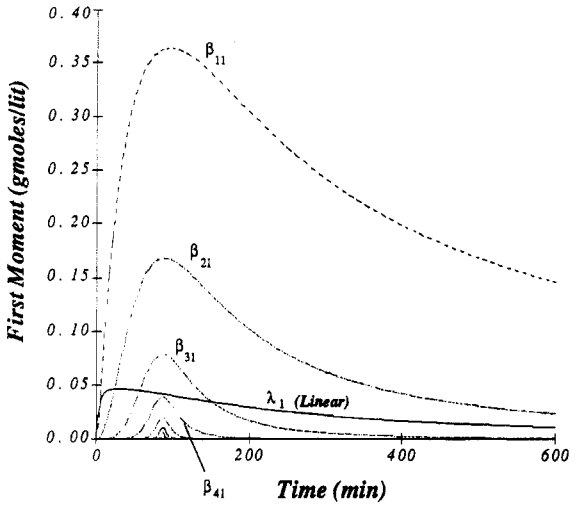

Figure 3. Time evolution of the first moment of the linear and branched generations for the base example case.

The method of overall moments tracks the evolution of the MWD moments without separating sol from gel; thus, it is limited to the calculation of the overall average molecular weights (or chain lengths), and only up to the gel point. The overall polymer second moment (and all subsequent moments) diverges at this point, and all calculations have to be stopped; calculation of postgel properties is impossible without the use of additional more complicated techniques.[11] In contrast, as the equations of our model are integrated in time, one can follow the progression of the moments of all the generations included, in both the pre- and postgel regimes. The dynamic behavior of these moments generally gives a good indication of the evolution of branching and gelation. If the first moment is examined, it reflects the relative amounts of polymer formed in each generation, thus resulting in an estimate of the level of branching. The amount of pseudogel formed is continuously calculated as the difference between the overall polymer first moment and the sum of the first moments of all generations. This difference is found to be numerically equal to zero up to the gel point, where it starts increasing, marking the sol/gel transition.

Figure 3 illustrates the behavior of the first moment of the linear polymer and all branched generations, while Figure 4 concentrates on the dynamics of a few of the higher generations (generations 4–10). It can be seen that these generations start appearing one after the other and that each generation does not start forming until enough polymer in the preceding generation has been produced. This is to be expected, since we have already postulated that each generation is used to build the next higher. However, one also has to notice that the first moment of each generation completely encloses the next higher (i.e., is formed before it but is consumed after it), which confirms the earlier statement about the transient nature of the higher generations. It can be seen that these keep appearing and growing up to the gel point and then are

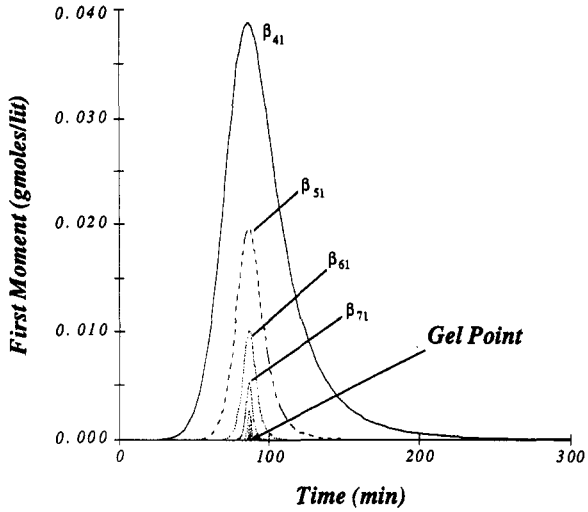

Figure 4. Time evolution of the first moment of the higher branched generations. Generations 4–10 are included. The gel point lies at the intersection of the locus of the maxima with the time axis.

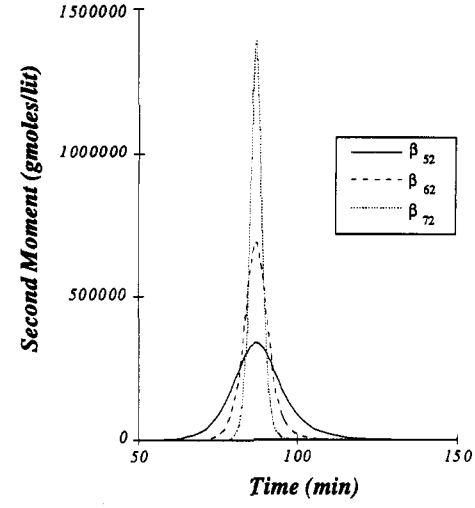

Figure 5. Time evolution of the second moment for generations 5–7.

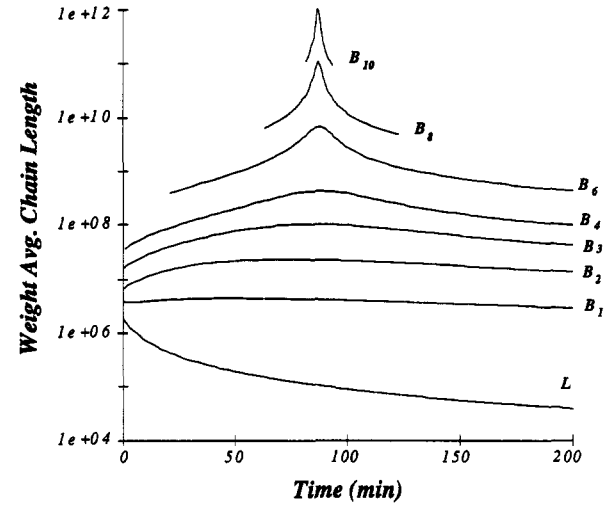

Figure 6. Time evolution of the weight-average chain length of various polymer generations.

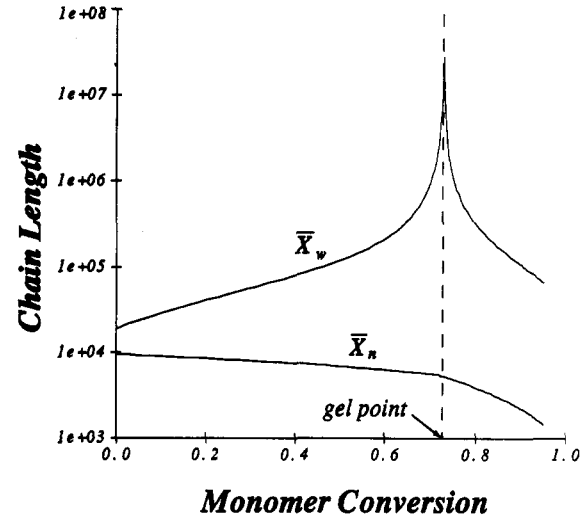

Figure 7. Number-average and weight-average chain length of the sol polymer plotted versus monomer conversion.

quickly consumed after. Shortly after the gel point only a few branched generations will coexist with the linear polymer (*cf.* Figure 3) and the newly formed gel (not shown). Thus, it can be seen that these higher generations form the first molecules of gel by extending the tail of the MWD toward very large molecular weights. After these first gel molecules are formed, the presence of higher generation polymer is no longer a necessity for the formation of additional gel, since the new gel polymer continues to grow by directly consuming polymer from all generations (in reality this occurs via a two-step mechanism where a dead polymer molecule is first activated by chain transfer and then terminates by combination with a gel molecule). As a result, the transformation of sol to gel continues to proceed even though a large gap in molecular weight exists between them. Another important implication of this transient nature is that the evolution of the MWD of a polymer system seeded with gel particles will be vastly different. If gel is added to the system before the higher generations are formed, these will never manage to exist, since they will be consumed faster than they can form. In consequence, no gel point will be encountered during the evolution of such a system, and the resulting sol polymer will generally possess a narrower and smoother MWD; however, some amount of gel will be present in the product stream.

In Figure 4, the exact location of the gel point can be found by the extrapolation of the locus of the maxima of the consecutive first moments to its intersection with the time axis. The behavior of the second moment is similar (Figure 5) but differs in the fact that successive generations achieve larger maxima in the second than in the first moment. The resulting physical situation is such that, as the generations appear, smaller amounts of larger polymer are being formed, again indicating the transient nature of these large molecules.

Another advantage of our modeling technique is that it allows the complete separation of sol from gel in the calculations. Thus, one can compute the average molecular weights of the sol polymer without succumbing to the numerical difficulties that inherently arise in the immediate vicinity of the gel point when the method of moments is used. Figure 6 illustrates the evolution of the weight-average chain length of the various generations, while Figure 7 presents the number- and weight-average chain length of the overall sol polymer. These have been plotted versus monomer conversion for the purpose of comparison with the results of Tobita and Hamielec.[10] The overall sol chain-length averages were calculated by summing the moments of all generations and then by computing the ratio of the first to zeroth moment and the second to first moment. In Figure 7, the decrease in both average chain lengths after the gel point is a result of the disappearance of the higher generations forming the high end of the

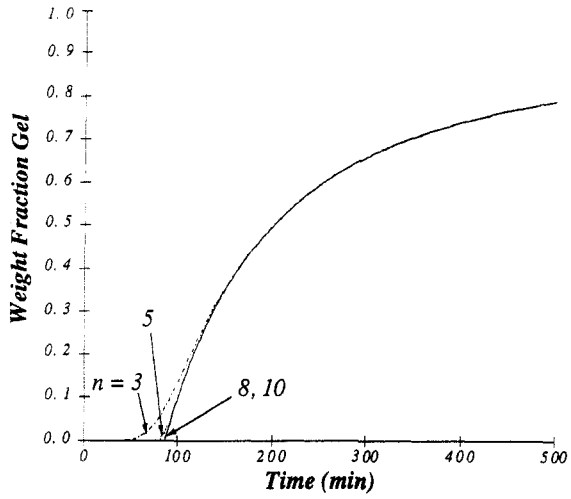

Figure 8. Evolution of the gel fraction calculated using different numbers of generations (n = 3, 5, 8, and 10).

molecular weight distribution.

The amount of gel formed can also be calculated as shown in Figure 8, where the gel fraction is plotted versus time. Different numbers of branched generations have been used in Figure 8 to illustrate the quick convergence of the method onto the true gel fraction curve. It can be seen that no difference is discernable whether 8 or 10 generations are used and that the use of 5 generations is generally sufficient.

The Molecular Weight Distribution. One of the most important capabilities of the modeling technique illustrated here is the ability to reconstruct the sol MWD. Methods based on the overall moments cannot accomplish this, since these do not separate sol from gel and can only result in a unimodal molecular weight distribution. This MWD keeps broadening with time up to the gel point where its polydispersity becomes very large. Because of its unimodal nature, the resulting MWD at this point will have the appearance of a flat curve extending across the molecular weight axis toward infinity. As detailed above, the actual behavior of the MWD in gelling systems is expected to be completely different, since the large increase in polydispersity near the gel point is associated with severe multimodality resulting from the rapid and successive formation of the higher polymer generations. Not only have we observed experimental evidence of such behavior in a proprietary system but some additional evidence was also found in the open literature. Schosseler et al.[23] have studied the cross-linking of polystyrene in solution initiated by radiolysis. They analyzed the MWD of the polymer at frequent intervals using size-exclusion chromatography (SEC) coupled with either refractometry or light scattering measurements. Their results (cf. Figures 1 and 2 in the cited reference) not only confirm the evolution scenario detailed above but also exhibit striking qualitative similarity with the MWD trends presented here later. This is not surprising since they conclude that, in their case, branching was caused by chain transfer to polymer and termination was mostly by combination, as in the example studied here. Charmot and Sauterey[24] also observed strongly multimodal gel permeation chromatography (GPC) traces for samples taken in the immediate vicinity of the gel point in their study of gelation in the emulsion polymerization of chloroprene. As attention is attracted to this phenomenon accompanying gelation, more evidence will be available in the literature; however, this behavior should not be confused with other MWD broadening effects usually associated with reactor effects or heterogeneities of the reaction medium. These only lead to weak multimodality (bi- or trimodal distributions) and are not associated with a divergence in polydispersity and hence are of a very different nature.

In reconstructing the sol MWD from the molecular weight moments, each set of moments for an individual generation is used in generating a distribution for that species; then all the distributions are summed according to their contributions to yield the overall MWD. The Schultz distribution,[25] which is a two-parameter distribution, is used to represent the individual generations. The weight fraction at a chain length x for the ith generation $W(x,i)$ is given by:

$$W(x,i) = \frac{y_i(xy_i)^{z_i}e^{-xy_i}}{\Gamma(z_i+1)} \tag{33}$$

where

$$z_i = \frac{1}{\left(\frac{\bar{x}_{w_i}}{\bar{x}_{n_i}} - 1\right)} \tag{34}$$

$$y_i = \frac{z_i + 1}{\bar{x}_{w_i}} \tag{35}$$

and $\bar{x}_{n_i}$ and $\bar{x}_{w_i}$ represent the number- and weight-average chain lengths of the ith generation. We should mention here that while we freely use the term MWD throughout the text, all results and calculations are based on chain-length distributions (CLD) which could be transformed into the former if multiplied by the molecular weight of the monomer.

The total CLD $W_t(x)$ is then obtained by summing the contributions of each generation according to the ratio of its first moment Q_{1_i} to the total first moment Q_{1_t}:

$$W_t(x) = \sum_{i=1}^{n} W(x,i)\frac{Q_{1_i}}{Q_{1_t}} \tag{36}$$

The CLD thus obtained is a "true" chain-length distribution and cannot be immediately compared to that measured by GPC, since the latter distorts the appearance of distributions containing branched polymers. In fact, GPC measures elution time which is proportional to the hydrodynamic volume of the polymer molecules. Since branched molecules are more compact, they will apparently reflect a smaller hydrodynamic volume and thus elute at an "apparent" shorter chain length. In order to correct for this effect, we have applied a correction term to all of the distributions calculated here, thus enabling a qualitative comparison with GPC traces. The correction is based on the assumption that the hydrodynamic volume of a linear polymer chain is proportional to x^3 (where x is the chain length), while that of a branched polymer chain is proportional to x^d, where d is the fractal dimension of the network. For simplicity, we have used one value of d for all branched polymers; in future applications, the dependence of d on the generation number could be investigated. The value used is the fractal dimension resulting from the chemical model for gelation,[26] which is approximately 1.8. The distributions were shifted to lower chain length by calculating the apparent CL from the true CL according to:

$$x^3_{\text{apparent}} = x^d_{\text{true}} \tag{37}$$

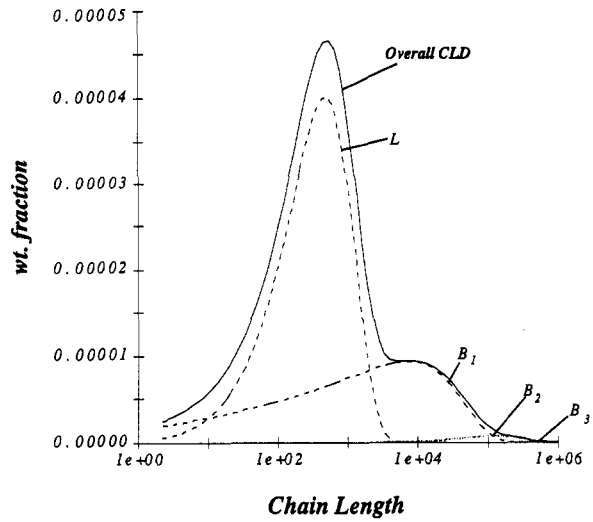

Figure 9. Overall chain-length distribution of the sol polymer at a reaction time t = 87 min, just prior to the gel point. Underlying individual distributions for the linear polymer and the first three branched polymer generations are shown scaled by their respective first moments.

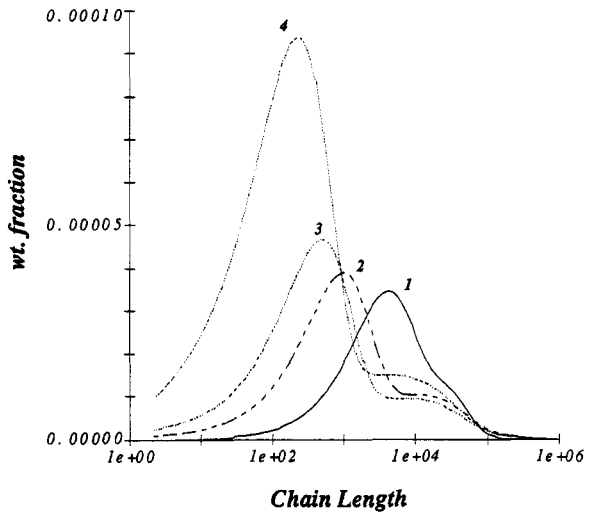

Figure 10. Evolution of the chain-length distribution, presented at reaction times t = 10, 50, 87, and 150 min. The gel point occurs between the last two times.

The ordinate values were then multiplied by $dx_{true}/dx_{apparent}$ for renormalization; as a result the distribution will be shifted to the left and its maximum will be elevated.

Figure 9 illustrates the reconstruction of the CLD at a reaction time just prior to the onset of gelation. Four individual generations are presented along with the overall CLD which shows two pronounced shoulders toward its high CL end. More shoulders and peaks are present in the tail area but can only be detected when viewed on a logarithmic scale. The scenario of evolution of the CLD described earlier is confirmed in Figures 10 and 11, where the overall CLD is plotted at four different sampling times. The first three distributions are of polymer in the pregel regime as they successively approach the gel point. The last distribution is for a time after gelation has occurred and represents the distribution of the sol polymer in the postgel regime. Although the main feature apparent in Figure 10 is a continuous shift of the linear generation peak toward lower chain lengths, the sol weight-average CL is continuously increasing as confirmed earlier. This effect is a known batch reactor effect, resulting from the decreased rate of propagation obtained as the monomer is depleted. The actual increase in the weight-average CL is due to the behavior of the high end of the distribution.

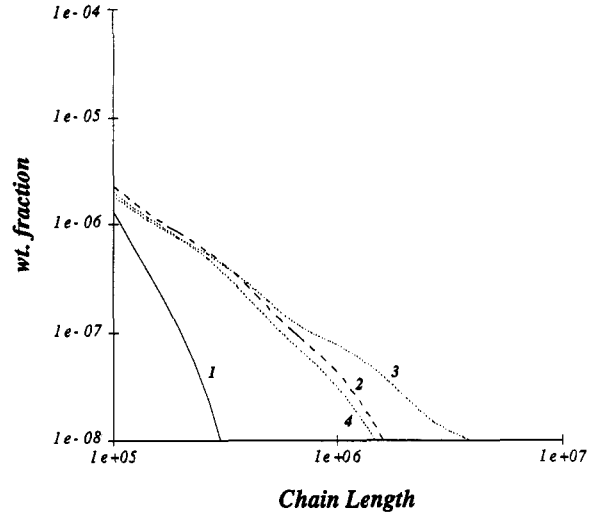

Figure 11. Enlargement of the tail ends of the distributions of Figure 10.

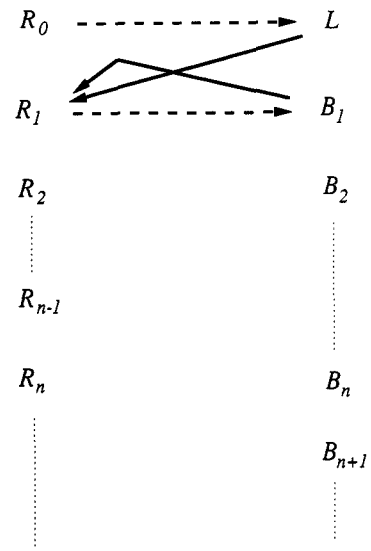

Figure 12. Generation transfer chart for the case where termination is solely by disproportionation. (→) Chain transfer to polymer. (- - →) Termination. In the absence of combination, no path can be established to the higher generations and gel.

This can be detected in Figure 11, where a logarithmic scale is used. The extension of the distribution's tail to higher chain lengths and the added shouldering can be seen for the first three curves, while the snap-back effect is seen for the fourth. Note that, as seen in Figure 10, the CLD at the last time (after the gel point) is still clearly multimodal and will continue to appear as such for a long time after gelation, despite the obvious narrowing it experiences.

Effect of the Termination Mechanism. Tobita and Hamielec[10] conclude, for the example used, that if, live radical termination is solely by disproportionation, gelation cannot occur. This is a fact that has been commonly accepted but never explained on a sound basis. The theory presented here offers a systematic approach for *a priori* determination of the possibility of gelation for any reaction mechanism. If a generation transfer chart is constructed as in Figure 12, one notices that in the absence of termination by combination no path exists that links the first branched polymer generation to the second. As a result, only linear and first-generation branched polymers can be made, and gelation is thus forbidden. The same conclusion can be reached via physical reasoning. If one thinks of a certain critical chain length necessary for gel to form, it can be seen that, in the absence of combination,

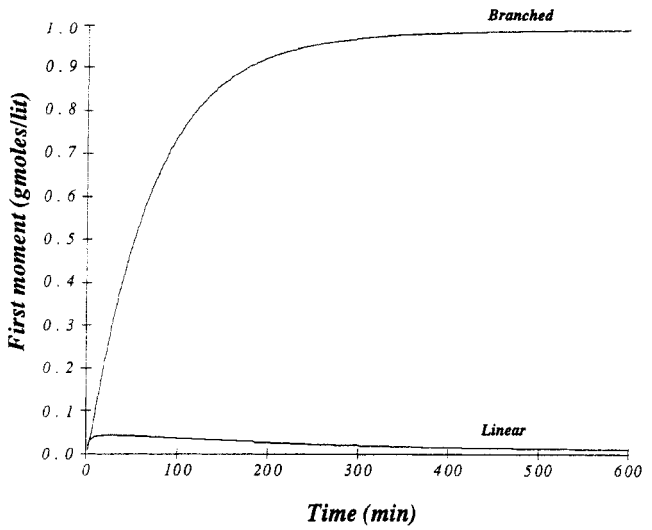

Figure 13. Evolution of the first moment for the case with no combination. Only linear and first-generation branched polymers exist.

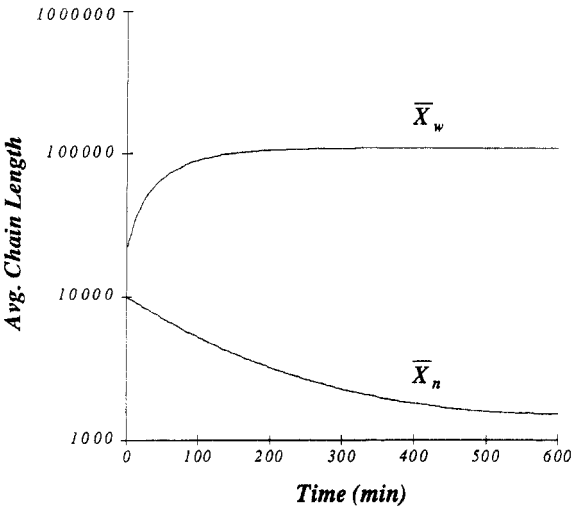

Figure 14. Evolution of the average chain lengths for the case of Figure 13. The distance between both curves increases with time, marking an increase in polydispersity.

the only instance where reaching this critical length is possible is when only one live radical exists per critical mass, and even then one has to assume that it can propagate to that length without terminating. Thus, in this case, gelation can only occur in the limit of zero initiator concentration, a highly theoretical limit. The physical significance in this example might be clear, but in more complex cases the generation transfer charts should provide a useful guide to the analysis of gelation.

Results obtained for the sample example, after termination by combination is turned off ($\beta_0 = 0$), are presented in Figures 13–15. In Figure 13, the first moments of linear and branched polymer are followed, showing that only two generations exist and that the degree of branching increases with time, resulting in a continuous increase in the weight-average chain length as seen in Figure 14. In this figure, it is also seen that the number-average CL continuously decreases as before and consequently very broad distributions will result. This is illustrated in Figure 15 where the CLD is reconstructed and reflects two distinct peaks. It can be concluded that, when termination is exclusively by disproportionation, gelation does not occur but very broad bimodal distributions can result.

It has to be said that this fact is only true if the assumptions of the model used hold. In our model, as

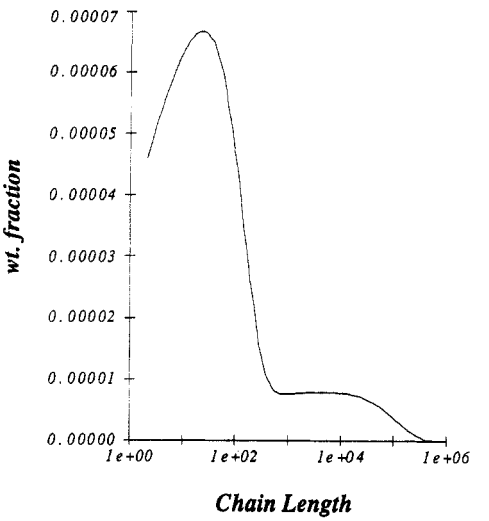

Figure 15. Chain-length distribution for the case of Figure 13 at a reaction time of t = 600 min.

well as in Tobita and Hamielec's, the rate of terminal double-bond polymerization has been assumed negligible. This is usually a good assumption for terminal double bonds created by disproportionation, which are known to be relatively inactive. However, if that rate happens to be appreciable, then gelation can theoretically occur, since this reaction will allow a branched live radical to "connect" to another branched dead polymer, thus resulting in a live radical in the next higher generation. A path leading to a pseudogel can thus be established and might lead to gelation.

Additional Capabilities. This paper has concentrated on demonstrating some of the capabilities of the method presented, especially those that were not achieved by other methods. It has to be realized that, since the method is kinetic in principle and is based on the method of moments, it can compute a host of other polymer properties and characteristics and include various reaction limitations. It even offers the added advantage of calculating these properties for individual generations, not just for the overall polymer. Examples of other properties that can be computed are branching moments, cross-link densities, and their distributions. Additional effects that can be included in the model are the dependence of rate constants on polymer structure (as reflected by generation number), intrachain cyclization for vinyl/divinyl systems, multiple radicals on a single molecule, and others. Diffusion limitations and their effect on rate constants can also be added to the model when necessary. These limitations are known to reduce the rate of termination to a larger extent than they would other reaction steps, which will in turn greatly alter the characteristics of the sol/gel transition in any particular system.

Conclusions

The technique presented here not only overcomes the general numerical difficulties associated with the use of the kinetic method of moments in analyzing gelling systems but also offers an insight into the nature of the sol/gel transition. The theory explains why a broadening in the MWD of the sol polymer is seen before gelation while narrowing occurs afterward. The model is continuous through the gel point and is easily adaptable for any mechanism of branching and/or cross-linking. A host of polymer properties can be computed using this method; these include the sol properties in the pregel and postgel regimes, the gel fraction, and the location of the gel point. A complete description of the molecular weight of the sol

polymer is also achieved and leads to the reconstruction of the molecular weight distribution, which is shown to be highly multimodal in the vicinity of the gel point. This feature of gelation has been frequently overlooked as a result of the fast rise and fall of the polymer polydispersity but should be stressed as an inherent feature of gelation. Most importantly, the method offers a systematic method of discerning the potential for gelation of any kinetic scheme, based on whether the transfer between generations will or will not proceed. This was applied to an example case in which chain transfer to polymer occurs and the termination mechanism was assumed to proceed via either combination or disproportionation. The theory explains why gelation is possible for the former and not the latter.

Acknowledgment. We are grateful to Professors A. E. Hamielec and W. H. Ray for their valuable comments and discussion. F.T. would like to acknowledge the generous support of S. C. Johnson Polymer during his postdoctoral tenure in Racine, WI.

References and Notes

(1) Flory, P. J. *J. Am. Chem. Soc.* **1941**, *63*, 3083.
(2) Stockmayer, W. H. *J. Chem. Phys.* **1943**, *11*, 45.
(3) Gordon, M. *Proc. R. Soc. London* **1962**, *268*, 240.
(4) Macosko, C. W.; Miller, D. R. *Macromolecules* **1976**, *9*, 199.
(5) Dotson, N. A.; Galvan, R.; Macosko, C. W. *Macromolecules* **1988**, *21*, 2560.
(6) Scranton, A. B.; Peppas, N. A. *J. Polym. Sci., Part A: Polym. Chem.* **1990**, *28*, 39.
(7) Bamford, C. H.; Tompa, H. *Trans. Faraday Soc.* **1954**, *50*, 1097.
(8) Saidel, G. M.; Katz, S. *J. Polym. Sci., Polym. Phys. Ed.* **1968**, *6*, 1149.
(9) Nagasubramanian, K.; Graessley, W. W. *Chem. Eng. Sci.* **1970**, *25*, 1549.
(10) Tobita, H.; Hamielec, A. E. *Makromol. Chem., Makromol. Symp.* **1988**, *20/21*, 501.
(11) Tobita, H.; Hamielec, A. E. *Macromolecules* **1989**, *22*, 3098.
(12) Charmot, D.; Guillot, J. *Polymer* **1992**, *33*, 352.
(13) Stauffer, D. *J. Chem. Soc., Faraday Trans.* **1976**, *72*, 1354.
(14) Rushton, A. F.; Family, F.; Herrmann, H. J. *J. Polym. Sci., Polym. Symp.* **1985**, *73*, 1.
(15) Bansil, H. J.; Herrmann, H. J.; Stauffer, D. *J. Polym. Sci., Polym. Symp.* **1985**, *73*, 175.
(16) Matthew-Morgan, D.; Landau, D. P.; Herrmann, J. *Am. Phys. Soc., Phys. Rev.* **1984**, *29*, 6328.
(17) Herrmann, H. J.; Stauffer, D.; Landau, D. P. *J. Phys. A* **1983**, *16*, 1221.
(18) Mikes, J.; Dusek, K. *Macromolecules* **1982**, *15*, 93.
(19) Bowman, C. N.; Peppas, N. A. *Chem. Eng. Sci.* **1992**, *47*, 1411.
(20) Teymour, F.; Campbell, J. D. *DECHEMA-Monogr.* **1992**, *127*, 149.
(21) Popplewell, L. M.; Campanella, O. H.; Peleg, M. *Chem. Eng. Prog.* **1989**, *9*, 56.
(22) Petzold, L. R. *DASSL, A Software Package for the Solution of Differential/Algebraic Systems of Equations*; Sandia National Laboratories: Livermore, CA, 1983.
(23) Schosseler, F.; Benoit, H.; Grubisic-Gallot, Z.; Strazielle, C. L.; Lieber, L. *Macromolecules* **1989**, *22*, 400.
(24) Charmot, D.; Sauterey, F. *DECHEMA-Monogr.* **1992**, *127*, 483.
(25) Billmeyer, F. W. *Textbook of Polymer Science*; Wiley-Interscience: New York, 1962.
(26) Julien, R.; Botet R. *Aggregation and Fractal Aggregates*; World Scientific; Singapore, 1986.